Effects of Flame Structure and Hydrodynamics on Soot Particle Inception and Flame Extinction in Diffusion Flames

R. L. Axelbaum, R. Chen, *Washington University, St. Louis, MO USA*
P. B. Sunderland (NCMR), D. L. Urban, *NASA Glenn Research Center, Cleveland, OH USA*
S. Liu and B. H. Chao, *University of Hawaii, Hawaii, USA*

INTRODUCTION

This paper summarizes recent studies of the effects of stoichiometric mixture fraction (structure) and hydrodynamics on soot particle inception and flame extinction in diffusion flames. Microgravity experiments are uniquely suited for these studies because, unlike normal gravity experiments, they allow structural and hydrodynamic effects to be independently studied. As part of this recent flight definition program, microgravity studies have been performed in the 2.2 second drop tower. Normal gravity counterflow studies also have been employed and analytical and numerical models have been developed.

A goal of this program is to develop sufficient understanding of the effects of flame structure that flames can be "designed" to specifications – consequently, the program name *Flame Design*. In other words, if a soot-free, strong, low temperature flame is required, can one produce such a flame by designing its structure? Certainly, as in any design, there will be constraints imposed by the properties of the available "materials." For hydrocarbon combustion, the base materials are fuel and air. Additives could be considered, but for this work only fuel, oxygen and nitrogen are considered. Also, the structure of these flames is "designed" by varying the stoichiometric mixture fraction. Following this line of reasoning, the studies described below are aimed at developing the understanding of flame structure that is needed to allow for optimum design.

SOOT INCEPTION

Recent experimental, numerical and analytical work has shown that the stoichiometric mixture fraction, Z_{st}, can have a profound effect on soot formation in diffusion flames [1-7]. This effect appears even at constant adiabatic flame temperature, T_{ad}, as demonstrated by Du and Axelbaum [1, 2]. An important finding of these works was that at sufficiently high Z_{st} the flames remain blue even when the strain rate approaches zero in counterflow flames, or as flame height and residence time approach infinity in coflowing flames. Lin and Faeth [4] coined the term *permanently blue* to describe such flames.

Flames considered in past studies involved counterflow and gas-jet configurations, which do not allow independent variation of flame structure and convection direction. Thus, it was not possible to assess the relative contributions of structure and hydrodynamics because both structure and hydrodynamics suppress soot formation at high Z_{st} in normal-gravity diffusion flames.

To better understand the mechanism responsible for permanently blue flames, the onset of luminous soot (the soot limit) was examined in spherical microgravity diffusion flames burning ethylene at atmospheric pressure. In a novel application of microgravity, spherical flames were employed to allow convection across the flame to be either from fuel-to-oxidizer or from oxidizer-to-fuel, while at the same time allowing Z_{st} to be independently varied. Stoichiometric mixture fraction was varied by changing

inert concentrations such that adiabatic flame temperature did not change [2]. Nitrogen was supplied with the oxidizer at low Z_{st} and with the fuel at high Z_{st}.

Thus motivated, we established four flames: (a) ethylene issuing into air, (b) diluted ethylene issuing into oxygen, (c) air issuing into ethylene, and (d) oxygen issuing into diluted ethylene. The stoichiometric mixture fraction for flames (a) and (c) is 0.064 and for flames (b) and (d) it is 0.78. Under the assumption of equal diffusivities of all species and heat, the stoichiometric contours of the flames have identical nitrogen concentrations and adiabatic temperatures.

The experiments were conducted in the NASA Glenn 2.2-second drop tower using a general-purpose combustion rig. The burner is a 6.4 mm diameter porous sphere consisting of sintered 10 micron stainless steel particles. Temperatures were measured using an uncoated Pt/Pt-Rh thermocouple and were corrected for radiation losses.

Since the drop tower provides only 2.2 seconds of microgravity time, a transient theoretical model was developed to evaluate the effects of unsteadiness and heat loss on the temperatures of the flames. The model adopts a simplified single-step, flame-sheet approximation for reaction chemistry and a detailed modeling of heat loss. Radiative heat losses from the gas and the burner surface are included. The optically thin model is adopted to formulate the gas radiation.

Figure 1 shows color images, captured just prior to drop termination, of representative flames for the four conditions considered. Each flame has an ethylene consumption rate of 1.5 mg/s and an adiabatic flame temperature of 2370 K. Figure 2 shows predicted flame and burner temperatures for the four flames of Fig. 1. The numerical results show that after ignition the flame temperature increases, approaching an asymptote in tens of seconds. None of the flames has reached steady state within the 2.2 seconds of drop time. Furthermore, although the adiabatic flame temperatures of all four flames are the same, the flame temperatures vary considerably. In particular, Flames (a) and (d) are substantially cooler and evolve more slowly than Flames (b) and (c). The agreement between theory and experiment is only fair, presumably due to the optically thin radiation assumption used in the model.

Structure is seen to have a significant effect on soot formation in the present flames, yielding permanently blue flames when Z_{st} is increased to 0.78. The permanently blue state is realized in Fig. 1d despite unfavorable hydrodynamics, where convection is towards the fuel. Flames (a) and (d) have almost identical measured temperatures and similar theoretical temperatures. Convection favors soot oxidation in Flame (a) and soot formation in Flame (d). Nonetheless, Flame (a) produces soot while Flame (d) does not, indicating that flame structure is responsible for the soot free conditions of Fig. 1d. Furthermore, the flame in Fig. 1b, which has $Z_{st} = 0.78$, is soot free.

The results of this study support the importance of flame structure on soot inception and permanently blue conditions. Nonetheless, the transient nature of the problem, as demonstrated by the numerical calculations, indicates that there are uncertainties. Microgravity tests in gas-jet flames indicate that steady soot concentrations require test times exceeding those of ground-based facilities. Furthermore, in the present brief tests, thermophoresis may cause soot formed during ignition to be trapped within the flame. Thus, longer microgravity test times are required and are being pursued.

FLAME EXTINCTION

The effects of Z_{st} on extinction of methane counterflow diffusion flames are shown in Figure 3, where numerical predictions of scalar dissipation rate at extinction (as characterized by $(\nabla Z)^2$ at Z_{st}) are plotted as a function of Z_{st}. Counterflow experiments have been performed to verify the model but are

not included here. The profound impact of Z_{st} is evident, with an almost 40 fold increase in scalar dissipation rate with Z_{st}. Furthermore, the flame temperature at extinction can be 140 °C lower when Z_{st} is increased from $Z_{st} = 0.055$ (methane/air) to 0.65. The minimum flame temperature at extinction occurs at the peak in scalar dissipation rate indicating that the flames at $Z_{st} = 0.65$ are very strong. This result is due to the shift in the oxygen profile into the high temperature region of the flame and the resulting increase in radical production, shown in Figs. 4 and 5. At $Z_{st} = 0.65$ the radical production region is coincident with the peak temperature, as seen in Fig. 5. For methane burning in air (Fig. 4) this is not the case and consequently much higher flame temperatures are required to sustain the flame. This interesting finding suggests that the $Z_{st} = 0.65$ flame is a better designed flame in that it more efficiently uses the high temperature of the flame for radical production.

This work was supported by NASA Grants NCC3-697, NAG3-1910, NCC3-696a,and NAG3-1912, with D. P. Stocker serving as Project Scientist. The assistance of S. A. Gokoglu, B. J. Goldstein, J. E. Pierce and H. D. Ross is duly appreciated.

REFERENCES

1. Du, J . and Axelbaum, R. L., *Combust. Flame* 100:367 (1995).
2. Du, J., and Axelbaum, R. L., *Proc. Combust. Inst.* 26:1137 (1996).
3. Chao, B. H., Liu, S. and Axelbaum, R. L., *Combust. Sci. Tech.* 138:105 (1998).
4. Lin, K. -C. and Faeth, G. M., *J. Prop. Power* 12:691 (1996).
5. Lin, K. -C. and Faeth, G. M., *J. Prop. Power* 12:10 (1996).
6. Lin, K. -C. and Faeth, G. M., *Combust. Flame* 115:468 (1998).
7. Sugiyama, G., *Proc. Combust. Inst.* 25:601 (1994).
8. Sunderland, P. B., Köylü, Ü. Ö., and Faeth, G. M., *Combust. Flame* 100:310 (1995).

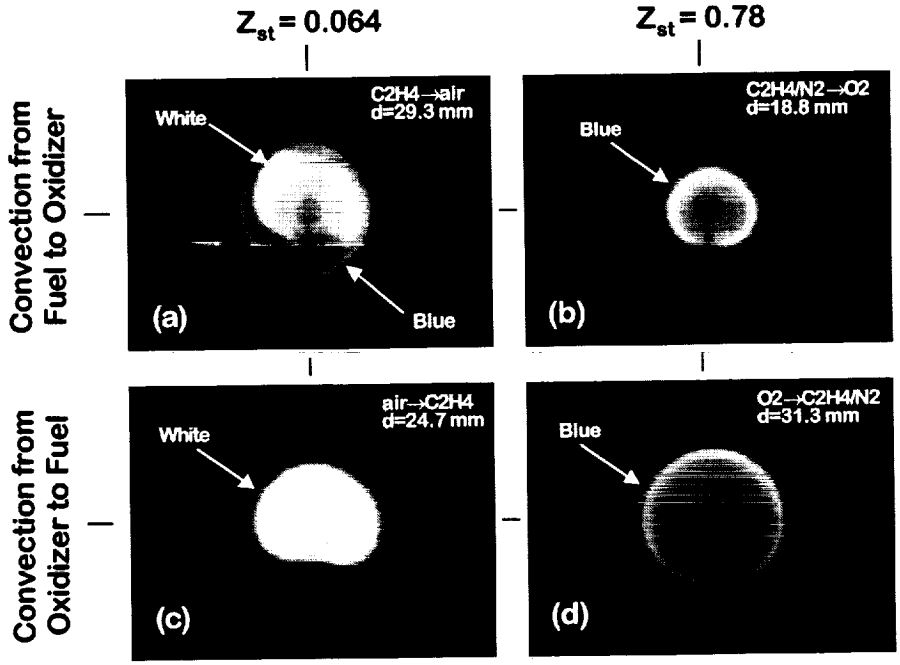

Fig. 1 Images of representative flames at the end of the 2.2 second drop: (a) ethylene (1.51 mg/s) issuing into air, f1.4; (b) diluted ethylene (19 mg/s) issuing into oxygen, f1.4; (c) air (22 mg/s) issuing into ethylene, f6; (d) oxygen (5.2 mg/s) issuing into diluted ethylene, f6. The scale is revealed by the 6.4 mm spherical burner. The ethylene consumption rate is 1.51 mg/s in all cases.

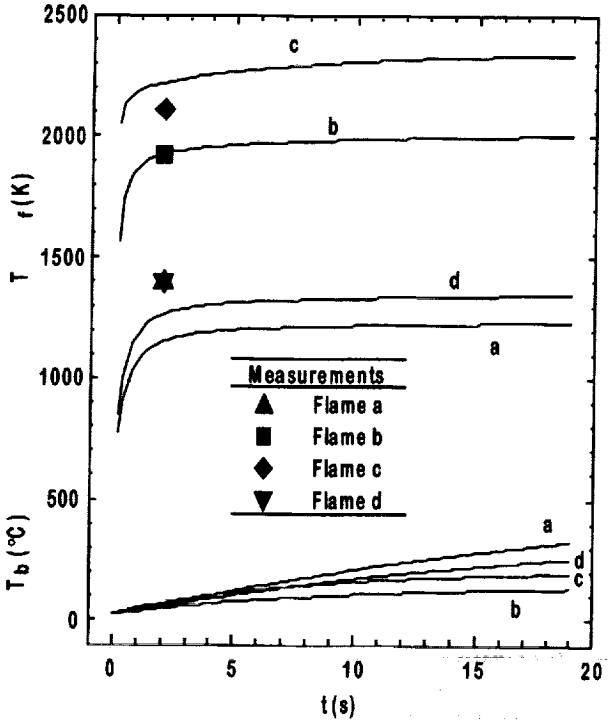

Fig. 2. Predicted flame temperature and burner temperature for flames (a) – (d). Also shown, by symbols, are measured peak temperatures after 2.2 s.

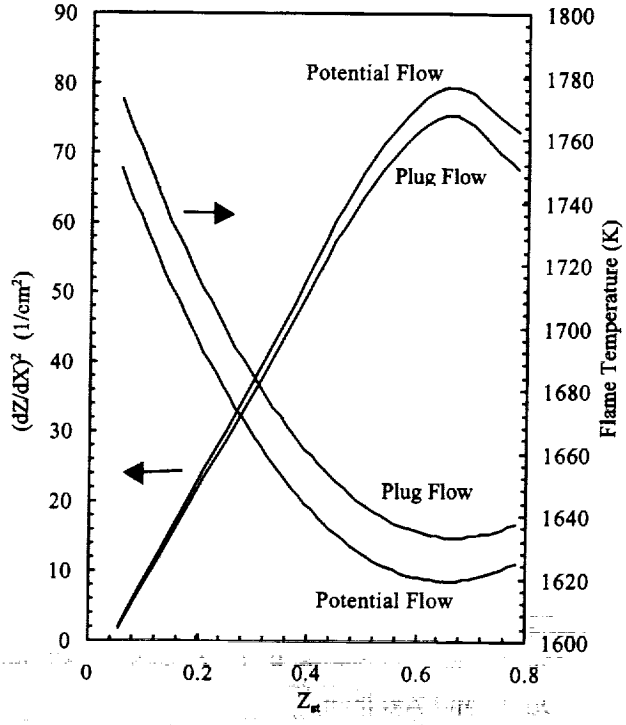

Fig. 3. Scalar dissipation rate (as characterized by $(\nabla Z)^2$ at Z_{st}) and flame temperature at extinction for methane.

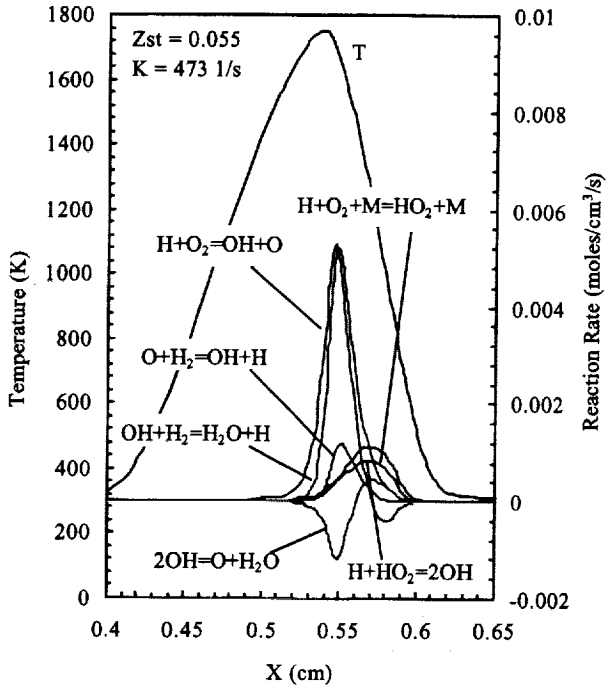

Fig. 4. Radical production rates and flame temperature distributions for a methane flame with $Z_{st} = 0.055$.

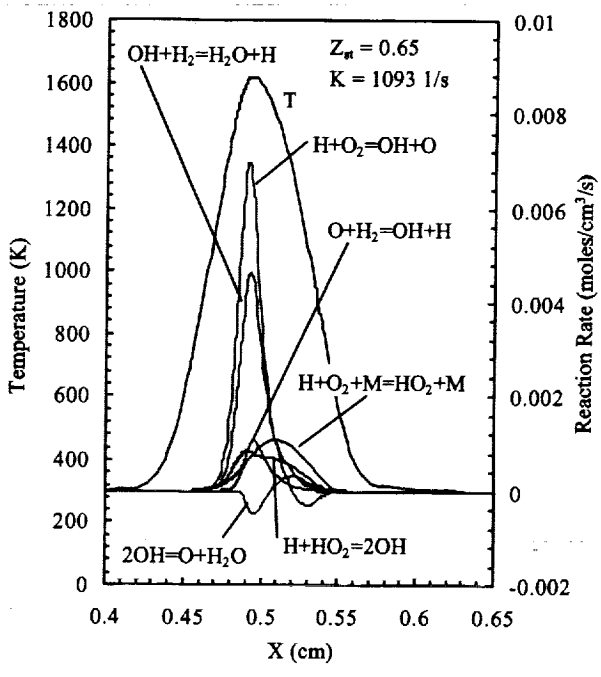

Fig. 5. Radical production rates and flame temperature distributions for a methane flame with $Z_{st} = 0.65$.